

The mechanism of cytotoxicity of methylmercury: Inhibition of progression through the S phase of the cell cycle

Edward J Massaro

Center for Biochemical Engineering, Duke University, Durham, NC 27706, USA, and US EPA Health Effects Research Laboratory, Research Triangle Park, NC, USA

The effect of methylmercury (MeHg) on progression of the murine erythroleukemic cell (MELC) through the cell cycle was analyzed by flow cytometry (FCM). Exposure *in vitro* to 5.0–10.0 $\mu\text{mol dm}^{-3}$ MeHg for 6 h resulted in a dose-dependent decrease in the rate of cell replication, apparently as a result of inhibition of DNA synthesis (rate of passage through the S phase of the cell cycle). Thus, only a modest accumulation of cells with a G_2/M ($4n$) DNA content was observed. At or above 10 $\mu\text{mol dm}^{-3}$ MeHg, progression through all phases of the cell cycle was blocked. FCM revealed a dose-dependent increase in cellular refractive index (90° light scatter), decrease in apparent cell volume (axial light loss), and increase in resistance to non-ionic detergent (NP-40)-mediated cytolysis indicative of fixation (protein denaturation, cross-linking, etc.) of the plasma membrane/cytoplasm complex. The data indicate DNA synthesis as the primary target of MeHg cytotoxicity.

Keywords: Methylmercury, cytotoxicity, DNA synthesis, murine erythroleukemic cell

INTRODUCTION

Methylmercury (MeHg), a ubiquitous contaminant of the aqueous environment,¹ is a potent neurotoxin and teratogen.^{2–5} Apparently, the mechanism of MeHg cytotoxicity is complex. It has been reported that MeHg inhibits mitosis and/or decreases the rate of the cell cycle. Mitotic arrest appears to result from inhibition of microtubule assembly,^{6–9} while decreased cycling rate has been attributed to lengthening of the duration

of the G_1 phase of the cell cycle as a consequence of inhibition of protein synthesis.¹⁰ Whether the duration of other pre-mitotic phases of the cell cycle is altered is not clear. However, it has been observed that MeHg inhibits DNA, RNA, and protein synthesis,^{5,11} interacts with the cytoskeleton,^{8,12} alters the properties of biomembranes,^{5,13–15} and disrupt axoplasmic transport.¹⁶

By flow cytometry (FCM), we have observed that MeHg perturbs the cell cycle kinetics of the murine erythroleukemic cell (MELC). At relatively low levels (5.0 $\mu\text{mol dm}^{-3}$), MeHg predominantly inhibits DNA synthesis (i.e. progression through the S phase of the cell cycle). Only a modest accumulation of cells with a $4n$ DNA content (i.e. in the G_2/M phase of the cycle as defined by FCM) is observed. At higher concentrations ($\geq 10 \mu\text{mol dm}^{-3}$), progression through all phases of the cell cycle is blocked. Light microscopy reveals a dose-dependent increase in the incidence of chromosomal aberrations. Chromosomal condensation is observed for doses $< 10 \mu\text{mol dm}^{-3}$. At 10 $\mu\text{mol dm}^{-3}$ MeHg, both condensation and pulverization are observed. Higher dose levels ($\geq 25 \mu\text{mol dm}^{-3}$) induce the formation of wreath-like chromosomal ring structures and progressive perturbation of the cell membrane/cytoplasm complex. The latter is manifested as increased 90° light scatter (refractive index,¹⁷ protein content¹⁸), decreased axial light loss (apparent cell volume, cell size¹⁹), simultaneous propidium iodide (PI) and carboxy-fluorescein (CF) fluorescence, and resistance to detergent (NP-40)-mediated cytolysis.²⁰ Our observations indicate that DNA synthesis is the primary target of MeHg cytotoxicity and that apparent targets and degree of cytotoxicity are a complex function of dose.

MATERIALS AND METHODS

Cells

Friend murine erythroleukemic cells (T3CL2; from Dr. Clyde Hutchinson, University of North Carolina, Chapel Hill) were grown in suspension culture in RPMI 1640 (Gibco, Grand Island, NY) supplemented with 10% fetal bovine serum (FBS) and 25 mmol dm⁻³ Hepes (Sigma, St Louis, MO, USA; no. H3375). Cell density was monitored by Coulter Counter (Model ZBI; Coulter Electronics, Inc., Hialeah, FL, USA) and the cells were passed every two to three days to maintain logarithmic growth.

Viability assay

Viability was estimated by FCM employing the carboxyfluorescein diacetate (CFDA; Molecular Probes, Eugene, OR, USA)/propidium iodide (PI; Sigma; no. P5264) assay.^{17,20,21}

Preparation of nuclei for cell cycle analysis

Logarithmically growing cells were harvested and washed as described previously.²⁰ Nuclei were isolated by non-ionic detergent [Nonidet P-40 (NP-40); Sigma; no. N6507]-mediated solubilization of the plasma membrane/cytoplasm complex and stained with fluorescein isothiocyanate (FITC; Sigma; no. F7250) for protein content and PI for DNA content.²⁰

Flow cytometry

Cytometric analyses were accomplished as described previously.^{18,20,22}

MeHg exposure protocol

Methylmercury(II) chloride (Alfa Inorganics, Danvers, MA, USA; no. 37123) in methanol was added to logarithmically growing MELC to final concentrations of 0.1, 0.25, 0.5, 1.0, 2.5, 7.5, 10, 25, or 50 $\mu\text{mol dm}^{-3}$. The final methanol concentration of the medium was 0.1% (no effect on viability or growth rate). Duration of exposure was 1, 2, 4, or 6 h. To investigate recoverability from the effects of MeHg exposure, cells were exposed to MeHg for 6 h, washed in prewarmed (37 °C) FBS-supplemented medium and reincubated for 18 h in MeHg-free medium.

Progression assay

The relative rate of movement of cells through the FCM-defined compartments of the cell cycle was estimated by a modification of the stathmokinetic assay of Darzynkiewicz *et al.*²³ which is based on the rate of accumulation of cells in the G₂/M phase of the cell cycle following treatment with Colcemid. Quantification of the phase distribution of cells was obtained with Multicycle, a cell cycle analysis PC software package (Phoenix Flow Systems, San Diego, CA, USA).

Quantification of the mitotic fraction of G₂/M nuclei

To estimate the percentage of cells in the M phase of the cell cycle, nuclei were prepared (from 1×10^6 cells per sample) according to the method of Pollack *et al.*,²⁴ which allows flow-cytometric discrimination of the M subpopulation.¹⁸

Chromosome morphology

Cells (1×10^6 per sample) were washed twice with phosphate-buffered saline (PBS; Sigma; no. 4417) by centrifugation (120 g, 5 min), resuspended in 10 cm³ of 75 mmol dm⁻³ potassium chloride and fixed in methanol-acetic acid (3:1). Chromosome spreads were prepared by centrifugation ($\sim 2 \times 10^4$ fixed cells, 500 g for 10 min at room temperature) onto glass slides in Leif cytobuckets (Coulter kit no. 322; Coulter Electronics, Inc., Hialeah, FL, USA), drying at 56 °C, and staining with 6% Giemsa (Sigma; no. G5637). The percentage of normal and abnormal chromosomes were obtained from 200 mitotic figures. The mitotic index was obtained from 500 cells. The data represent the mean \pm standard deviation of three experiments.

Data analysis

The data reported are from representative experiments. The experiments were repeated at least three times. For each cytometric parameter investigated (PI or FITC fluorescence, 90° light scatter, axial light loss), the distribution or mean of 10^4 events (cells or nuclei) per condition (dose, duration of exposure) or combination of conditions was determined. Data derived from cells exposed to MeHg concentrations below 2.5 $\mu\text{mol dm}^{-3}$ did not differ from the control condition and are not included.

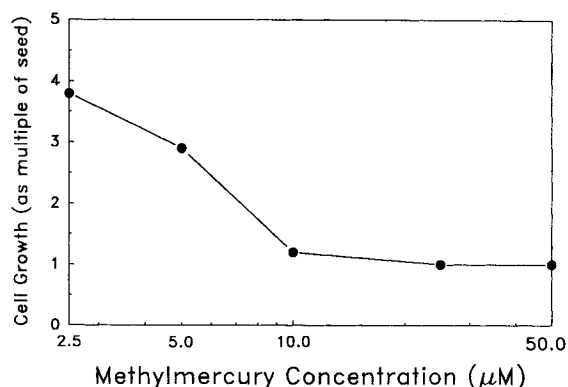


Figure 1 Rate of MELC growth following MeHg exposure (6 h), washout and reincubation (18 h) in MeHg-free medium. MELC doubling time after exposure to $2.5 \mu\text{mol dm}^{-3}$ MeHg was essentially equal to that of control cells.

$$\text{Multiple of seed} = \frac{\text{No. of cells at } T_{18}}{\text{No. of cells at } T_0}$$

where T_0 = time of inoculation of medium. T_{18} = 18 h post-inoculation.

RESULTS

Exposure of MELC to $\text{MeHg} \leq 5 \mu\text{mol dm}^{-3}$ for six hours or more has no significant effect on viability (estimated by the CFDA/PI assay: Table 1), 90° light scatter (see Fig. 7, below), a measure of protein content,¹⁸ or axial light loss (cell size¹⁷). However, rate of cell replication is decreased (Fig. 1) following MeHg washout and reincubation for 18 h in fresh, MeHg-free medium. Exposure to higher doses results in significant loss of viability (Table 1). At or above $5 \mu\text{mol dm}^{-3}$, MeHg alters the percentage distribution of cells across the cell cycle (Figs 2–6). Following exposure to $5 \mu\text{mol dm}^{-3}$ MeHg, DNA histogram analysis (Fig. 3: no Colcemid) reveals depletion of the G_0/G_1 compartment, increase in the percentage of cells in S phase (to a relatively steady state), and no increase in G_2/M compared with control cells, suggesting little movement of cells out of the S phase. Compared with control cells treated with Colcemid, addition of Colcemid to the $5.0 \mu\text{mol dm}^{-3}$ MeHg-treated cells has little, if any, affect on the percentage of G_2/M cells. If the primary effect of MeHg were on microtubule assembly/disassembly (a Colcemid-like effect) and S phase progression were normal, cells would accumulate in the G_2/M phase of the cycle at the expense of the other phases. Apparently, cells treated with MeHg can enter the S phase, but the rate at which they traverse this compartment is retarded, resulting in reduction of the rate of

influx of cells into G_2/M . Compared with control cells, exposure to $10 \mu\text{mol dm}^{-3}$ MeHg results in an increased percentage of cells in the S phase of the cycle and a slightly decreased percentage in G_0/G_1 and G_2/M . Exposure of such cells to Colcemid has minimal effect on phase distribution, indicating essentially complete cessation of cycling.

Eighteen hours after MeHg washout and reincubation under standard conditions, the DNA histogram of nuclei obtained from MELC exposed to $2.5 \mu\text{mol dm}^{-3}$ MeHg appears identical to that of control cells (Fig. 4). Also, the DNA histogram obtained from MELC exposed to $5 \mu\text{mol dm}^{-3}$ MeHg indicates considerable recovery toward a pattern of DNA distribution similar to that of logarithmically growing cells (compare Fig. 4 with Fig. 2), although there is persistent reduction of the rate of S phase traverse as evidenced by the accumulation of cells in early and mid S phase and depletion of cells in late S and the G_2/M phase. Colcemid treatment confirms recovery of normal cell cycle kinetics by cells exposed to $2.5 \mu\text{mol dm}^{-3}$ MeHg and persistence of S phase retardation in cells exposed to $5 \mu\text{mol dm}^{-3}$ MeHg. Reincubation of MELC exposed to doses $\geq 10 \mu\text{mol dm}^{-3}$ MeHg reveals a greatly perturbed DNA histogram manifesting an increased amount of debris, indicative of severe, irreversible cytotoxicity (data not shown).

The time-dependent effects of exposure to $5.0 \mu\text{mol dm}^{-3}$ MeHg or $0.2 \mu\text{g cm}^{-3}$ Colcemid on cell cycle progression are compared in Figs 5 and 6. By inhibiting mitosis, Colcemid exposure results in a relatively rapid increase in the percentage of cells in the G_2/M phase of the cell cycle at the expense of the G_0/G_1 and S phases (Fig. 6, open symbols). In contrast, the G_2/M compartment of MeHg-exposed cells increases only slightly and at a relatively slow rate over the course of the experiment; the S compartment increases to a maximum at 2 h and remains constant; and the G_0/G_1 compartment decreases to a minimum at 4 h. Also, in contrast to Colcemid exposure, the MeHg-exposed cells accumulate maximally in the S phase of the cycle.

To gain insight into the effect of MeHg on the G_2/M phase of the cell cycle, nuclei were prepared from MELC by an isolation procedure that allows flow cytometric discrimination of mitotic nuclei.^{18,42} On a contour cytogram of 90° scatter versus PI fluorescence (Fig. 7), M phase nuclei appear as a distinct subpopulation exhibiting decreased 90° scatter and PI fluorescence compared

Table 1 The mitotic index and percentage of chromosomal aberrations occurring after 6 h exposure to 0–50 $\mu\text{mol dm}^{-3}$ MeHg or 0.2 $\mu\text{g cm}^{-3}$ Colcemid.

MeHg dose ($\mu\text{mol dm}^{-3}$)	Viability (%)	Mitotics (%)	Chromosomal aberrations			
			Normal (%)	Condensed (%)	Pulverized (%)	Rings (%)
Control	98	3.1 ± 1.0	92 ± 6	5 ± 2	—	3 ± 4
2.5	98	4.2 ± 2.0	84 ± 8	13 ± 8	2 ± 2	2 ± 2
5.0	95	5.0 ± 0.9	74 ± 22	22 ± 15	4 ± 4	—
10.0	14	4.8 ± 3.0	3 ± 4	30 ± 34	12 ± 9	55 ± 41
25.0	3	4.5 ± 0.8	—	—	—	100 ± 0
50.0	5	3.9 ± 1.8	—	—	—	100 ± 0
Colcemid	97	41 ± 0	90 ± 4	10 ± 4	—	—

with G_2 nuclei. Following 6 h exposure to concentrations of $\text{MeHg} \leq 7.5 \mu\text{mol dm}^{-3}$, the percentage of cells in G_2/M remains relatively constant over dose (control-16.4%; $2.5 \mu\text{mol dm}^{-3}$ MeHg-14.7%; $5 \mu\text{mol dm}^{-3}$ MeHg-18.2%; $7.5 \mu\text{mol}$

dm^{-3} MeHg-19.4%). However, the contribution of the M subcompartment increases considerably. This suggests that, although progression from S phase into G_2 is retarded, subsequent progression from G_2 into M occurs. However, the percentage of cells exhibiting recognizable chromosomes does not increase substantially as a function of dose (Table 1), suggesting that cells leaving G_2 become arrested in a premitotic phase in which their nuclei exhibit the same biophysical properties as those of M phase cells but chromosome morphology is disrupted.

Chromosome analysis reveals an increase in the percentage of condensed and pulverized chromosomes (Table 1) and a modest increase in the mitotic index (considerably less than that caused by Colcemid) as a function of MeHg dose. At $10 \mu\text{mol dm}^{-3}$ MeHg, chromosome spreading was inhibited and the chromosomes of more than half of the mitotic cells appeared in the form of wreath-like ring structures (Table 1). Following

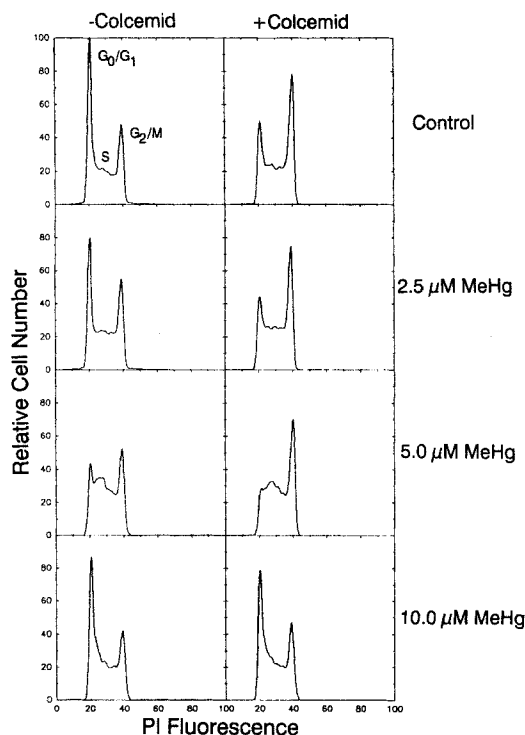


Figure 2 Representative DNA histograms of nuclei of MELC exposed to MeHg for 6 h with or without Colcemid for the last 2 h of exposure (progression assay). G_0/G_1 represents the pre-DNA synthetic phase of the cell cycle; S, the phase of DNA synthesis; G_2 , the post-synthetic phase preceding mitosis; and M, mitosis. Following exposure to $5.0 \mu\text{mol dm}^{-3}$ MeHg, movement of cells through the S phase of the cycle appears to be retarded. At $10 \mu\text{mol dm}^{-3}$ MeHg, there is complete cessation of cycling.

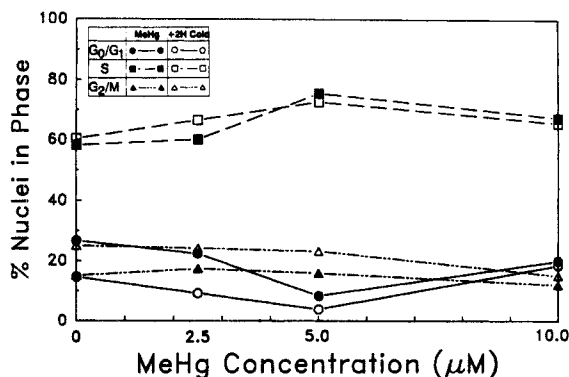


Figure 3 The percentage of cells in each cell cycle phase was determined by computerized mathematical analysis of the histograms of Fig. 2. Data points at $T=0$ depict the control condition. +2H Colc = exposure to Colcemid for 2 h (see Fig. 2).

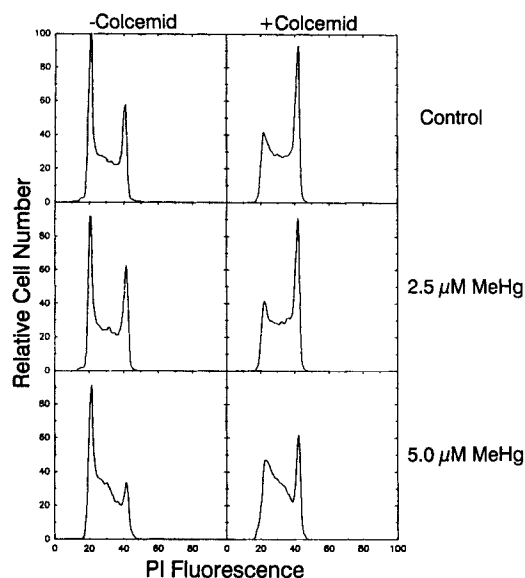


Figure 4 Representative DNA histograms of nuclei obtained from MeHg-exposed (6 h) MELC reincubated in MeHg-free medium for 18 h. The cell cycle distribution of cells recovering from exposure to $5.0 \mu\text{mol dm}^{-3}$ MeHg approaches normality, but still indicates retardation of progression into, through, and out of the S phase.

exposure to 25 or $50 \mu\text{mol dm}^{-3}$ MeHg for as little as 1 h (the shortest time period investigated), all spreads appeared in the form of wreath-like ring structures (Fig. 8).

DISCUSSION

The mechanism through which MeHg exerts its cytotoxicity has been postulated to involve binding to sulfhydryl groups and disruption of disulfide bonds. Indeed, inhibition of microtubule assembly, disruption of assembled microtubules, and inhibition of mitosis have been attributed to the binding of MeHg to sulfhydryl groups of tubulin.⁶⁻⁹ It is expected that sulfhydryl binding would also affect other cellular functions, including the structure and function of biomembranes and the cytoskeleton; synthesis, repair and structure of DNA, RNA (and, therefore, the cell cycle); protein synthesis, turnover, structure and function; and chromosome structure and function.^{5, 8, 11-16}

Cell cycle analysis (by FCM) reveals that MeHg induces a dose dependent increase in the percentage of cells in the S phase, little change in the

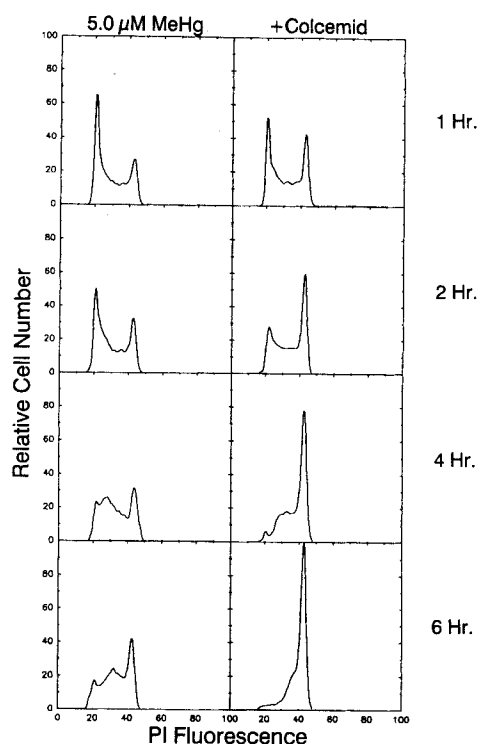


Figure 5 Exposure to Colcemid ($0.2 \mu\text{g cm}^{-3}$) results in time-dependent accumulation of cells in the G_2/M compartment and a sequential depletion of the G_0/G_1 and S compartments. In contrast, exposure to $5 \mu\text{mol dm}^{-3}$ MeHg results in accumulation of cells in the S phase and retardation of the rate of efflux out of this compartment. As a result, the G_0/G_1 compartment becomes depleted and accumulation of cells in the G_2/M compartment is inhibited.

percentage of cells in the G_2/M compartment compared with the control condition, and depletion of the G_0/G_1 compartment (Figs 2, 3, 5, and

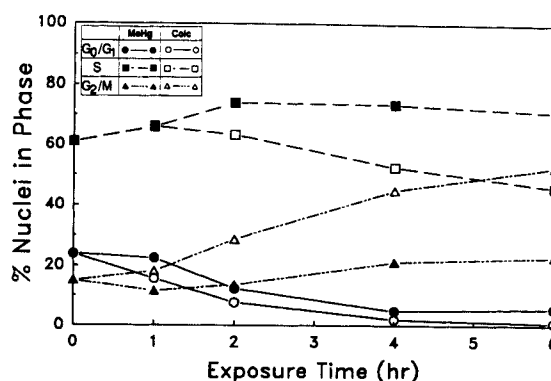


Figure 6 Computerized mathematical analysis of the histograms of Fig. 5. MELC were exposed to either $5 \mu\text{mol dm}^{-3}$ MeHg (filled symbols) or $0.2 \mu\text{g cm}^{-3}$ Colcemid (open symbols) as described in the text.

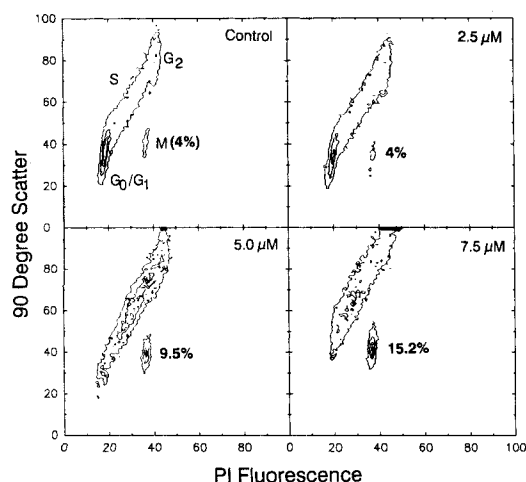


Figure 7 Contour cytograms of the 90° scatters versus PI fluorescence of nuclei isolated from MeHg-exposed (6 h) MELC by treatment with Pollack's buffer.²⁴ Mitotic nuclei appear as a distinct subpopulation exhibiting decreased 90° light scatter and PI fluorescence. Following MeHg exposure, the relative percentage of cells in this phase increases with dose.

6). Depletion of the G_0/G_1 compartment indicates retardation/inhibition of mitosis. Ordinarily retardation/inhibition of mitosis results in an increase in the size of the G_2/M compartment (a colchicine-like effect). That this is not observed indicates retardation of S phase transit, which is supported by the increase in the size of the S compartment (Figs. 2, 3, 5, and 6). However, cells exposed to concentrations of MeHg up to $5 \mu\text{mol dm}^{-3}$ exhibit partial, if not complete, recovery from these effects following reincubation in MeHg-free medium (Fig. 4).

To obtain more precise information on cell cycle effects, we investigated the time course of interaction of MeHg ($5 \mu\text{mol dm}^{-3}$) with logarithmically growing MELC (Figs 5 and 6). Computerized mathematical analysis of the DNA histogram indicates that the percentage of cells in the S phase increases with time, reaching a maximum after 2 h of exposure and remaining constant thereafter (Figs 5 and 6). At the same time, the percentage of cells in G_0/G_1 decreases and continues to decrease as a function of exposure up to 4 h, indicating reduction of the rate of influx of cells into this compartment. The percentage of cells in G_2/M changes little during the course of the experiment, suggesting (in the light of the S phase build-up) retardation of influx into and efflux out of this compartment (the size of the

G_2/M compartment is limited by the relative rates of S phase efflux and mitosis).

Increasing the MeHg dose to $10 \mu\text{mol dm}^{-3}$ does not increase the size of the G_2/M compartment (Figs 2 and 3). If the primary effect of MeHg is microtubule disruption, increasing the MeHg dose below the cytotoxic level would be expected to inhibit mitosis progressively, increasing the percentage of cells in the G_2/M compartment and the mitotic index. However, this is not the case (Figs 2 and 3; Table 1). Indeed, cells accumulate in the S compartment.

Quantification of the relative contribution of M phase cells to the G_2/M compartment (Fig. 7) reveals that, although the percentage of cells in G_2/M changes little as a function of dose (Fig. 3), the M subpopulation appears to increase substantially following exposure to MeHg concentrations of more than $2.5 \mu\text{mol dm}^{-3}$. Thus, it would appear that, at concentrations of MeHg ($>2.5 \mu\text{mol dm}^{-3}$) above which influx into G_2 is retarded, efflux out of M (i.e. mitosis) is retarded to a greater extent. However, morphologic analysis reveals that the mitotic index changes little as a function of MeHg dose (Table 1). This suggests that the apparent increase in the percentage of M phase nuclei results from the cells leaving G_2 becoming arrested in a premitotic phase in which the nucleus exhibits biophysical properties similar to those of M phase nuclei. This argues against the hypothesis that the mitotic spindle (i.e. the microtubule) is the primary target of MeHg, as does our observation of only limited accumulation of cells in the G_2/M phase of the cell cycle—far less than that seen after treatment with Colcemid, an agent that specifically blocks microtubule assembly (Table 1).

Following exposure to concentrations of MeHg $\geq 10 \mu\text{mol dm}^{-3}$, viability decreases (Table 1), growth is completely inhibited (Fig. 1), and traverse through all phases of the cell cycle is blocked (Figs 2 and 3).

Cytologic examination reveals that MeHg exposure perturbs chromosome structure. At MeHg concentrations less than $10 \mu\text{mol dm}^{-3}$, condensation and pulverization are the predominant chromosomal aberrations observed (Table 1; Fig. 8). Exposure at or above $10 \mu\text{mol dm}^{-3}$ results in the induction of wreath-like chromosomal ring structures that appear to be formed by chromosomal fusion.

Although the mechanism of ring structure formation is unknown, direct interaction of MeHg with chromatin as well as perturbation of the

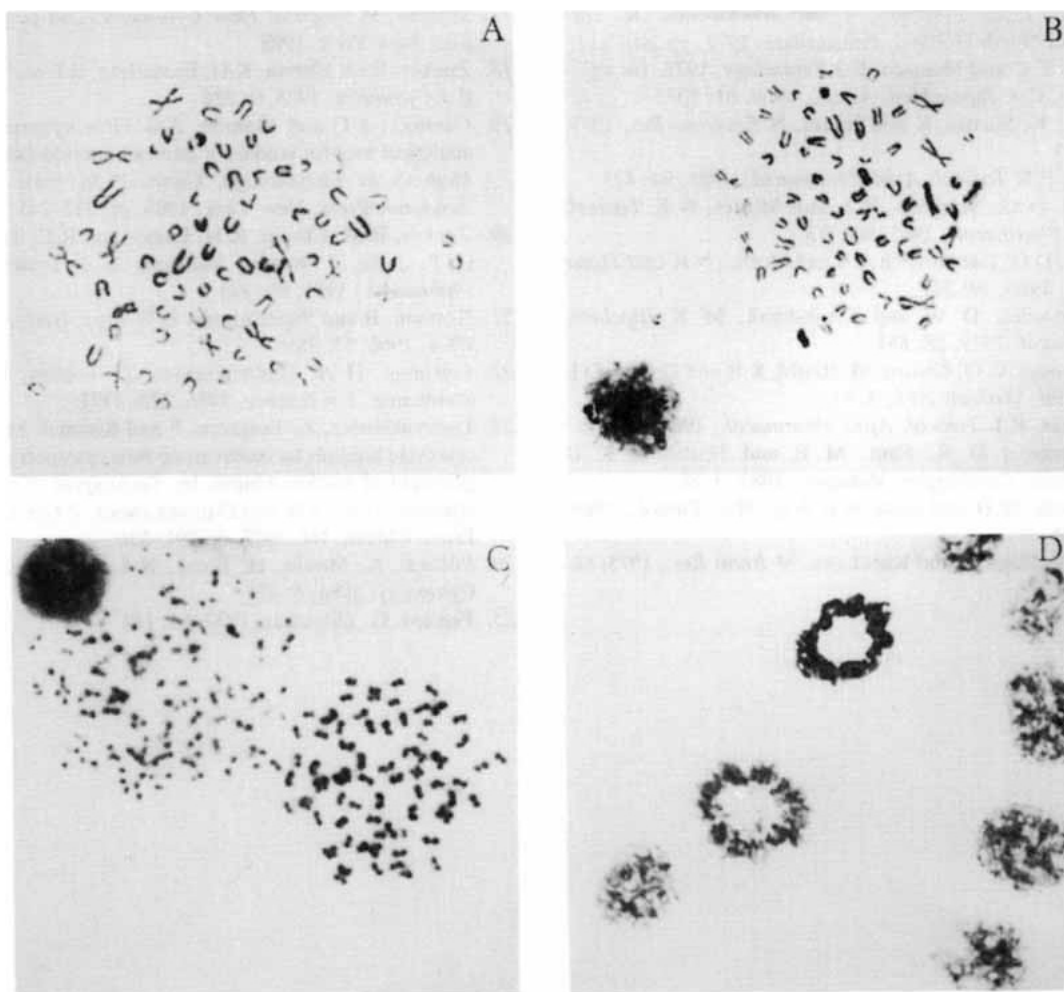


Figure 8 Representative photomicrographs (630 \times) of chromosomal aberrations induced by exposure (6 h) of MELC to MeHg. The chromosomes of cells exposed to 5 $\mu\text{mol dm}^{-3}$ MeHg (B) appear to be of normal morphology, but are smaller in size than those of control cells (A) and both cell growth (see Fig. 1) and S phase progression (see Figs 2–6) are inhibited. Following exposure to 10 $\mu\text{mol dm}^{-3}$ MeHg, condensed and/or pulverized chromosomes are observed (C). At or above 25 $\mu\text{mol dm}^{-3}$ Hg, the chromosomes appear in the form of wreath-like ring structures (D).

plasma membrane/cytoplasm complex resulting in alteration of the intracellular environment may be involved. It has been observed repeatedly that MeHg disrupts the structure/function of biomembranes (e.g., Refs 5, 13–15). Indeed, in cultured mouse neuroblastoma cells, Koerker¹³ reported that exposure to 1 $\mu\text{mol dm}^{-3}$ MeHg for 24–72 h at 37°C in Ham's F-12 medium supplemented with serum resulted in perturbation of the function of the plasma membrane, lysosomes, mitochondria, and endoplasmic reticulum.

REFERENCES

1. Mason, R P and Fitzgerald, W F *Nature (London)*, 1990, 347: 457
2. Geelen, J A, Dormans, J A and Verhoef, A *Acta Neuropathol. (Berlin)*, 1990, 80: 432
3. Amin-Zaki, L, Majeed, M A, Elhassani, S B, Clarkson, T W, Greenwood, M R and Doherty, R A *Am. J. Dis. Child.*, 1979, 133: 172
4. Harada, Y Congenital Minamata Disease. In: *Minimata Disease, Methylmercury Poisoning in Minimata and*

- Niigata, Japan (Tsubaki, T and Irkukayama, K, eds) Elsevier North Holland, Amsterdam, 1977, pp 209-239
5. Olson, F C and Massaro, E J *Teratology*, 1977, 16: 187
 6. Ramel, C J. *Japan Med. Assoc.*, 1969, 61: 1072
 7. Miura, K, Suzuki, K and Imura, N *Environ. Res.* 1978, 17: 453
 8. Sager, P R *Toxicol. Appl. Pharmacol.*, 1988, 94: 473
 9. Vogel, D G, Margolis, R L and Mottet, N K *Toxicol. Appl. Pharmacol.*, 1985, 80: 473
 10. Vogel, D G, Rabinovitch, P S and Mottet, N K *Cell Tissue Kinet.*, 1986, 19: 227
 11. Gruenwedel, D W and Cruikshank, M K *Biochem. Pharmacol.* 1979, 28: 651
 12. Wasteneys, G O, Cadrin, M, Reuhl, K R and Brown, D L *Cell Biol. Toxicol.* 1988, 4: 41
 13. Koerker, R L *Toxicol. Appl. Pharmacol.*, 1980, 53: 458
 14. Goodman, D R, Fant, M E and Harbison, K D *Teratogen. Carcinogen. Mutagen.*, 1983, 3: 89
 15. Peckham, N H and Choi, B H *Exp. Mol. Pathol.*, 1986, 44: 230
 16. Abe, T, Haga, T and Kurokawa, M *Brain Res.*, 1975, 86: 504
 17. Shapiro, H *Practical Flow Cytometry*, 2nd edn, Alan R Liss, New York, 1988
 18. Zucker, R M, Elstein, K H, Easterling, R E and Massaro, E J *Cytometry*, 1988, 9: 226
 19. Cambier, J C and Monroe, J G Flow cytometry as an analytical tool for studies of neuroendocrine function. In: *Methods in Enzymology*, Conn, P M (ed), vol. 103, Academic Press, New York, 1983, pp 227-245
 20. Zucker, R M, Elstein, K H, Easterling, R E, Ting-Beall, H P, Allis, J W and Massaro, E J *Toxicol. Appl. Pharmacol.*, 1989, 96: 393
 21. Rotman, B and Papermaster, B W *Proc. Natl. Acad. Sci. USA*, 1966, 55: 766
 22. Crissman, H A, Darzynkiewicz, Z, Topbey, R A and Steinkamp, J A *Science*, 1986, 228: 1321
 23. Darzynkiewicz, Z, Traganos, F and Kimmel, M Assay of cell cycle kinetics by multivariate flow cytometry using the principle of stathmokinesis In: *Techniques of Cell Cycle Analysis*, Gray, J W and Darzynkiewicz, Z (eds), Humana Press, Clifton, NJ, 1987, pp 291-336
 24. Pollack, A, Moulis, H, Block, N L and Irvin, G L III *Cytometry*, 1984, 5: 473
 25. Fiskejo, G, *Hereditas*, 1970, 64: 142